LA-UR-97-3737

Title:

The $\Lambda\Lambda$ interaction and the reaction $\Xi^{¾} + d \rightarrow n + \Lambda + \Lambda$

Author(s):

S. B. Carr
I.R. Afnan
B.F. Gibson

Submitted to:

http://lib-www.lanl.gov/la-pubs/00418741.pdf

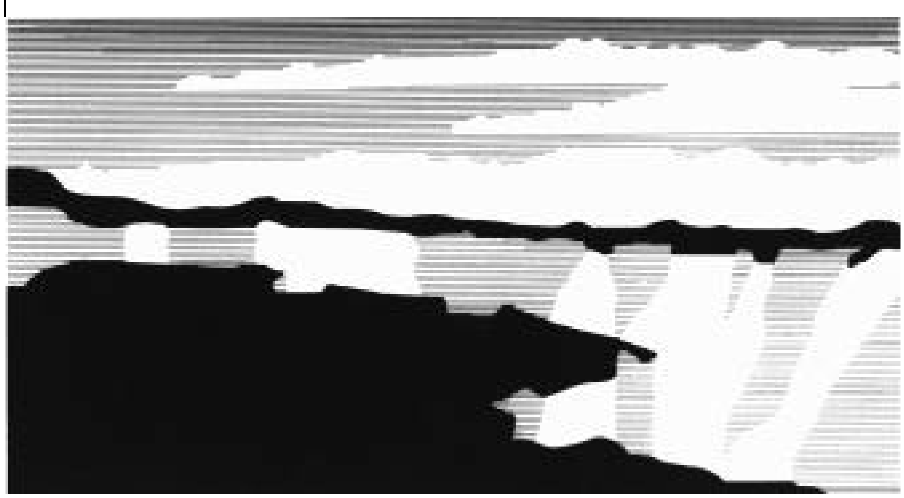

Los Alamos
NATIONAL LABORATORY

Los Alamos National Laboratory, an affirmative action/equal opportunity employer, is operated by the University of California for the U.S. Department of Energy under contract W-7405-ENG-36. By acceptance of this article, the publisher recognizes that the U.S. Government retains a nonexclusive, royalty-free license to publish or reproduce the published form of this contribution, or to allow others to do so, for U.S. Government purposes. The Los Alamos National Laboratory requests that the publisher identify this article as work performed under the auspices of the U.S. Department of Energy. Los Alamos National Laboratory strongly supports academic freedom and a researcher's right to publish; therefore, the Laboratory as an institution does not endorse the viewpoint of a publication or guarantee its technical correctness.

The $\Lambda\Lambda$ interaction and the reaction $\Xi^- + d \rightarrow n + \Lambda + \Lambda$ *

S. B. Carr[a], I. R. Afnan[a] and B. F. Gibson[b]

[a]Flinders University, South Australia

[b]Los Alamos National Laboratory, NM, U.S.A.

Interest in the $\Lambda\Lambda$ interaction is partly due to the presence of quark-model predictions for an $S=-2$ dibaryon [1], and partly to the interest in the role of the coupling between the $\Lambda\Lambda$ and ΞN channels in $\Lambda\Lambda$ hypernuclei [2]. This latter effect is expected to be substantially more important than the coupling of the NN to the $N\Delta$ channel in the $S=0$ sector, since the difference in threshold between the $\Lambda\Lambda$ and ΞN is only ≈25 MeV. In the absence of any direct measurement of the $\Lambda\Lambda$ amplitude, we must resort to either $\Lambda\Lambda$ hypernuclei, or to a reaction with a $\Lambda\Lambda$ final-state interaction to determine the YY (the $S=-2$ baryon-baryon system) interaction. In this report we present results of a theoretical study of the hypernucleus ${}^{6}_{\Lambda\Lambda}$He and the reaction $\Xi d \rightarrow n\Lambda\Lambda$ whereby we examine the sensitivity of the calculations to details of the $\Lambda\Lambda$ potential, and the coupling between the $\Lambda\Lambda$ and the ΞN channels.

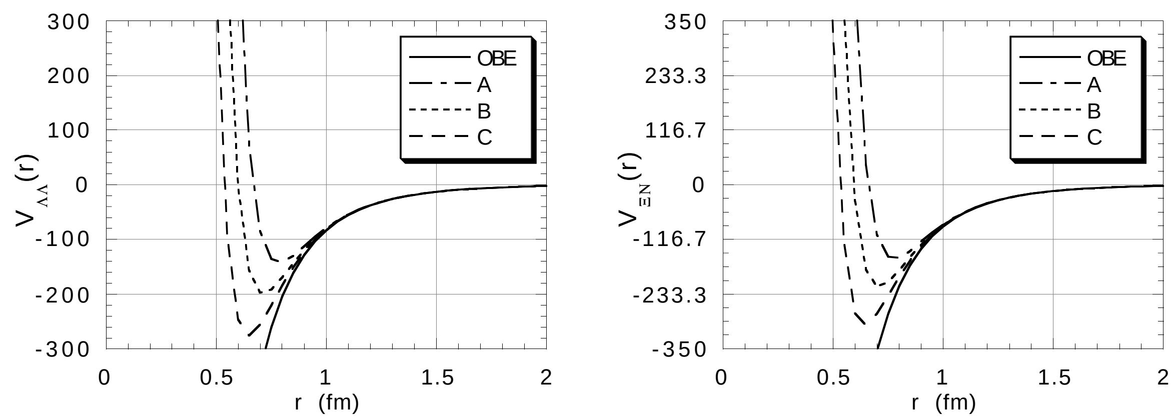

Figure 1. The ^{1}S$_0$ OBE $\Lambda\Lambda$ and ΞN potentials with and without short range repulsion.

In the absence of any data on the YY interaction, we have taken the meson exchange

*The authors would like to dedicate the present contribution to the memory of our friend and colleague Carl B. Dover who was instrumental in initiating this investigation.

part of the Nijmegen D potential for the NN system [3], and performed an $SU(3)$ rotation to determine the couplings of the mesons to the hyperons. For a purely S-wave interaction, the one boson exchange potential (OBEP) for the exchange of the $i^{\rm th}$ meson is given by

$$V_i(r) = V_c^{(i)}(r) + \vec{\sigma}_1 \cdot \vec{\sigma}_2 \; V_\sigma^{(i)}(r) \; . \tag{1}$$

Since the resulting OBEP is singular at the origin, we introduced a repulsive soft core with a cut-off mass $M \approx 2.5$ GeV. As a result the radial potential for the exchange of the $i^{\rm th}$ meson is:

$$V_\alpha^{(i)}(r) = V_0^{(i)} \left[\frac{e^{-m_i r}}{m_i r} - C \left(\frac{M}{m_i} \right) \frac{e^{-Mr}}{Mr} \right] \qquad \alpha = c, \sigma \; , \tag{2}$$

where m_i is the mass of the exchanged meson and $V_0^{(i)}$ is given in terms of masses and coupling constants as determined by the NN data [4,5]. The parameters M and C are adjusted to ensure that the long range part ($r > 0.8$ fm) of the meson exchange potential is not modified by the choice of cut-off. The final $\Lambda\Lambda$–ΞN interaction in the ^{1}S$_0$ channel has been chosen to either support a bound state (C), generate an anti-bound state (B), or have no bound state at all (A). In this way we can test the hypothesis that the ^{1}S$_0$ Λ–Λ interaction is comparable in strength to the ^{1}S$_0$ n–n potential [6]. In Fig. 1 we illustrate the diagonal elements of the coupled channel potentials and include the OBEP with no cut-off for comparison.

Table 1
The effective range parameters for the local and separable potentials in the ^{1}S$_0$ $\Lambda\Lambda$–ΞN.

Pot.	$a_{\Lambda\Lambda}$ (fm)	$r_{\Lambda\Lambda}$ (fm)	$a_{\Xi N}$ (fm)	$r_{\Xi N}$ (fm)	B.E. (MeV)
A	-1.91	3.36	-2.12-0.75i	3.45-0.45i	UB
SA	-1.90	3.33	-2.08-0.81i	3.44-0.22i	UB
B	-21.1	1.86	-2.05-6.53i	2.12-0.21i	UB
SB	-21.0	2.54	-2.07-6.52i	2.62-0.15i	UB
C1	7.82	1.41	3.08-5.26i	1.74-0.144i	0.71
SC1	7.84	1.48	3.05-5.28I	1.45+0.074I	0.71
C2	3.37	1.0	3.37-2.54i	1.44-0.10i	4.74
SC2	3.36	1.0	3.35-2.50i	1.83-0.09i	4.73

Since the above procedure gives a local coordinate space potential and because we propose to carry through a three-body calculation for the hypernucleus ${}_{\Lambda\Lambda}^{\;6}$He and the breakup reaction $\Xi^- d \rightarrow n\Lambda\Lambda$, we have constructed a set of S-wave separable potentials that give the same scattering length and effective range as the local potentials in the $S = -2$ sector. In Table 1 we present the effective range parameters in the ^{1}S$_0$ $\Lambda\Lambda$–ΞN channel for the local and separable potentials. Here we note that potential SA has no bound state, potential SB has a virtual or anti-bound state, while the potentials SC1 and SC2 give a binding energy of 0.71 and 4.74 MeV. To test the resulting potentials with the only piece of experimental data on the $\Lambda\Lambda$ interaction, we have calculated the binding energy of ${}_{\Lambda\Lambda}^{\;6}$He as a $\alpha\Lambda\Lambda$ three-body system using the Alt-Grassberger Sandhas equations

[7]. To examine the role of the coupling in the $\Lambda\Lambda$–ΞN channels, we have performed three distinct calculations by: (i) Including the coupling between the channels and solving the equation for the $\alpha\Lambda\Lambda$–$\alpha\Xi N$ system. (ii) Discarding the coupling between the channels without any modification to the parameters of the potential. (iii) Excluding the coupling between the channels, but adjusting the parameters to give the same $\Lambda\Lambda$ effective range parameters as the corresponding local potential. The results are presented in Table 2.

Table 2
The binding energy in MeV of ${}^{6}_{\Lambda\Lambda}$He for the four potentials under consideration.

	SA	SB	SC1	SC2	Exp.
$\alpha\Lambda\Lambda$ – $\alpha\Xi N$	9.738	12.268	15.912	19.836	
$\alpha\Lambda\Lambda$ with no coupling to $\alpha\Xi N$	9.508	11.606	14.533	17.508	10.9± 0.6
$\alpha\Lambda\Lambda$ with effective $\Lambda\Lambda$ potential	10.007	14.134	17.842	23.750	

If we compare these binding energies for ${}^{6}_{\Lambda\Lambda}$He with the one experimental measurement of 10.9 ± 0.6 MeV, we find that: (i) By comparing row one and three of Table 2, we may conclude that the inclusion of the coupling at the two-body level is essential if we are to avoid over-binding in heavier nuclei. (ii) From row one and two we observe that the contribution of the coupling between the $\Lambda\Lambda$ and ΞN in ${}^{6}_{\Lambda\Lambda}$He is small. This is due to the fact that the nucleon in the $\alpha\Xi N$ Hilbert space is Pauli blocked. (iii) The results in Table 2 suggest that the potential SB predicts the result closest to the experimental separation energy, and therefore best represents the $\Lambda\Lambda$ interaction. This supports the suggestion that the Λ–Λ ${}^{1}S_{0}$ interaction strength may in fact be comparable to that of the n–n ${}^{1}S_{0}$ interaction.

We now turn to the reaction $\Xi^{-}d \rightarrow n\Lambda\Lambda$ for which there is an experiment in progress at Brookhaven [8]. In the Fig. 2 we show the neutron differential energy spectrum (NDES) for this reaction for the four potentials under consideration. The energy at which the calculations have been performed corresponds to the Ξ^{-} capture by the deuteron at rest. With the exception of the result for the potential SB, the neutron spectrum does not exhibit the final state interaction (FSI) peak expected. In all four cross sections the dominant feature is the large broad peak at the low-energy end of the neutron spectrum.

A detailed investigation of the different contributions to the NDES reveals that the suppression of the FSI is the result of a destructive interference between the amplitudes that contribute to the NDES. In Fig. 3 we give a diagrammatic representation of the three amplitudes that contribute to the cross section. Diagrams (a) and (b) are expected to contribute to the FSI peak, since the final interaction is in the $\Lambda\Lambda$–ΞN coupled channels which for the potential SB is dominated by the anti-bound state pole. On the other hand, diagram (c) is a background term that could interfere constructively with either of the amplitudes corresponding to diagrams (a) and (b). To determine the relative sign of the three amplitudes we present in Figs. 4 and 5 the NDES for the diagrams (a) plus (c) and (b) plus (c) respectively. Here from the height of the FSI peak, we may conclude that diagrams (a) and (c) interfere destructively, while diagrams (b) and (c) give an enhancement in the FSI peak. This implies that diagrams (a) and (b) are out of phase.

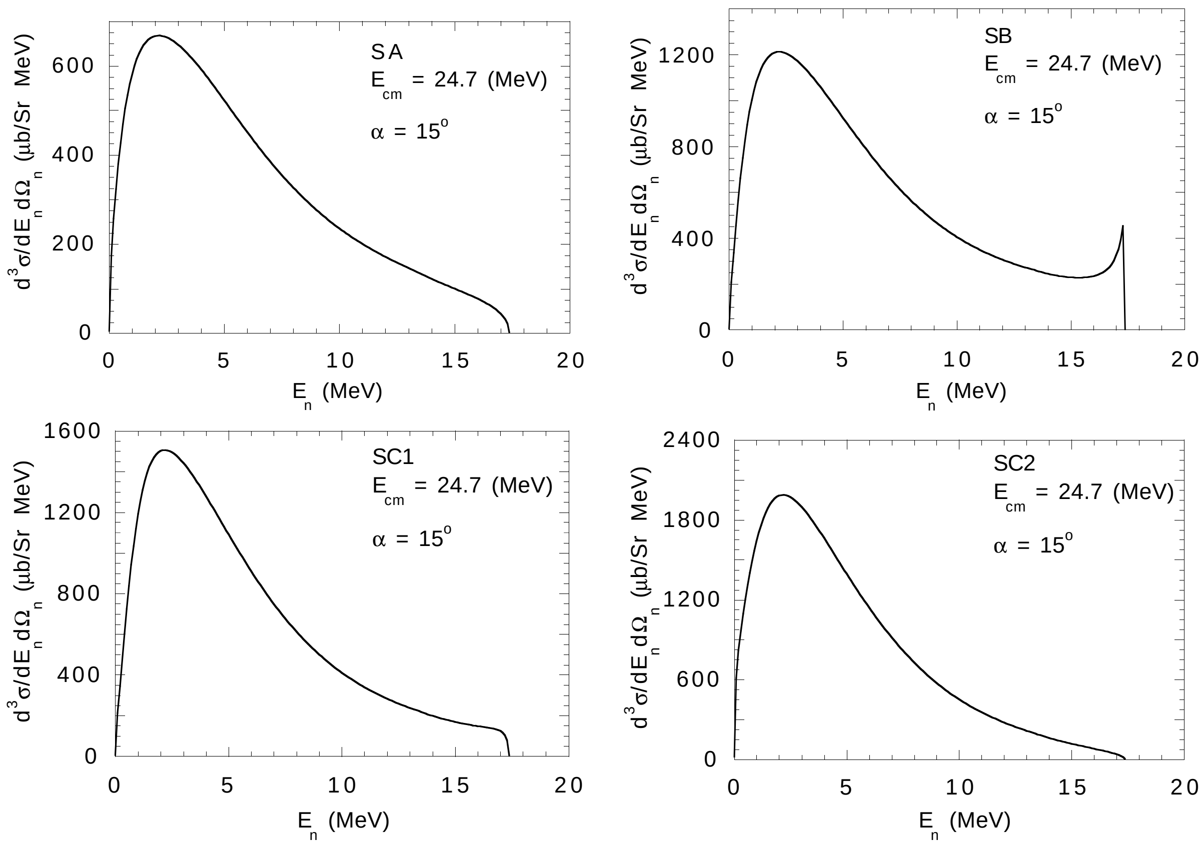

Figure 2. The NDES for the potentials SA, SB, SC1, and SC2.

Since both of these diagrams are dominated by the anti-bound state in the FSI region, the fact that they are out of phase implies that in the cross section the FSI peak is suppressed. This suppression of the FSI peak is purely the result of the fact that the final interaction is in the $\Lambda\Lambda$–ΞN coupled channel for which the diagonal $\Lambda\Lambda \leftarrow \Lambda\Lambda$ T-matrix is out of phase with the non-diagonal $\Lambda\Lambda \leftarrow \Xi N$ T-matrix and as a result we have a cancellation between diagrams (a) and (b). This is to be compared with the $n - d$ break-up where the final n–n interaction is a single channel ${}^1\mathrm{S}_0$ with a resultant enhancement in the FSI peak.

From Figs.s 4 and 5 we may also deduce that the broad peak at the low-energy end of the neutron spectrum comes from diagram (a). In lowest order, this is proportional to the momentum distribution of the neutron in the deuteron, *i.e.* the momentum space deuteron wave function. Since we used the same wave function with the four potentials under consideration, the shape of this peak in the NDES is the same for the four potential (see Fig. 2).

From the above results for the NDES we may conclude that in the event of an $S = -2$ dibaryon being present just below the $\Lambda\Lambda$ threshold, it would give rise to a clean signal not to be confused with a FSI peak.

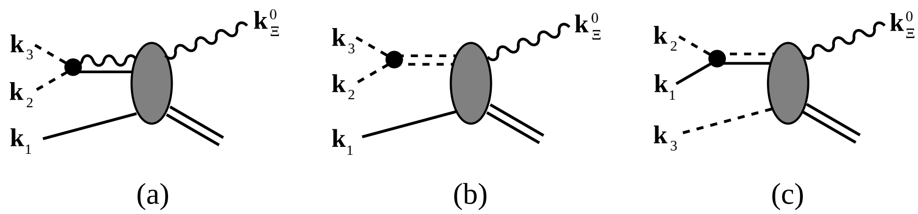

Figure 3. The three amplitudes that contribute to the NDES for $\Xi^- d \rightarrow n\Lambda\Lambda$.

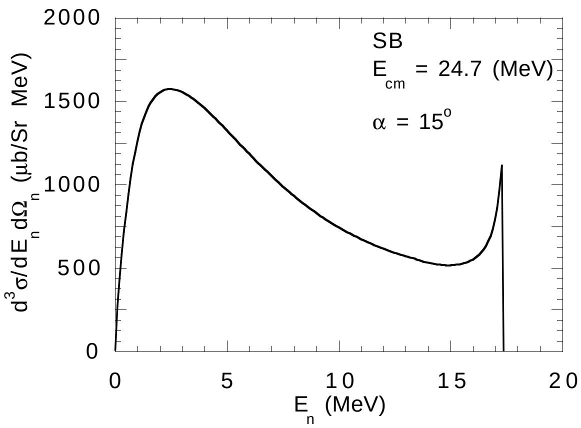

Figure 4. The NDES for (a) plus (c).

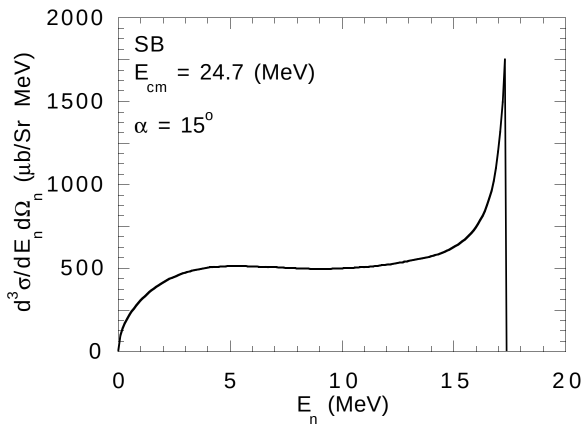

Figure 5. The NDES for (b) plus (c).

REFERENCES

1. R.L. Jaffe, Phys. Rev. Lett. **38** (1977) 195.
2. B.F. Gibson, *et al.*, Prog. Theor. Phys. Suppl. **117** (1994) 339.
3. M.M. Nagel, T.A. Rijken and J.J. de Swart, Phys. Rev. D **15** (1977) 2547.
4. S.B. Carr, Ph.D. Thesis, Flinders University (1996).
5. S.B. Carr, I.R. Afnan and B.F. Gibson, to be published in Nucl. Phys **A**.
6. C.B. Dover, private communication.
7. E.O. Alt, P. Grassberger and W. Sandhas, Nucl. Phys. **B2** (1967) 167.
8. P.D. Barnes, Nucl. Phys. **A547** (1992) 3c.